World Academy of Science, Engineering and Technology
International Journal of Mechanical and Mechatronics Engineering
Vol:6, No:8, 2012

Numerical Simulation of the Effects of Nanofluid on a Heat Pipe Thermal Performance

Barzin Gavtash, Khalid Hussain, Mohammad Layeghi, Saeed Sadeghi Lafmejani

***Abstract*—**This research aims at modeling and simulating the effects of nanofluids on cylindrical heat pipes thermal performance using the ANSYS-FLUENT CFD commercial software. The heat pipe outer wall temperature distribution, thermal resistance, liquid pressure and axial velocity in presence of suspended nano-scaled solid particle (i.e. Cu, Al2O3 and TiO2) within the fluid (water) were investigated. The effect of particle concentration and size were explored and it is concluded that the thermal performance of the heat pipe is improved when using nanofluid as the system working fluid. Additionally, it was observed that the thermal resistance of the heat pipe drops as the particle concentration level increases and particle radius decreases.

***Keywords*—**CFD, Heat Pipe, Nanofluid, Thermal resistance

I. Introduction

HEAT pipe is a device which operates in a closed loop two phase (vapour-liquid) thermodynamic cycle in order to transfer heat at high rates from one point to another with a very small change in the temperature along the pipe. Heat pipes are also known as one of the most effective passive heat transfer methods with high thermal conductivity [1].

A conventional heat pipe also referred as a cylindrical (circular) heat pipe with a constant conductance coefficient consists of a sealed container and a fully saturated annular porous wick material with working fluid, which is situated along the pipe. The basic principles of the heat pipe operation are based on the evaporation, mass transfer and condensation of the working fluid. The heat pipe is divided into three main zones; evaporator (heat-in zone), adiabatic (transport zone) and condenser (heat-out zone) as shown in Fig. 1.

When heat is applied to the evaporator end of the pipe, it is radially conducted into the container wall as well as the wick and causes the working fluid of the wick to vaporize. Due to a partial vacuum inside the pipe, the working fluid can be transformed into vapour for temperature much less than the phase change which normally happens at atmospheric pressure. This additional resultant vapour mass cause an increase in the vapour pressure in the evaporator and the subsequent pressure deferential provides a thrust force through which the vapour moves to the condenser section via the adiabatic channel. In the condenser zone the latent heat of vaporization is removed from the flow by taking advantage of a heat sink and hence condensation occurs.

B. Gavtash was with the Mechanical Engineering Department of Bradford University, UK, BD7 1DP (phone: +44 (0)7834 728 924; e-mail: barzin4@yahoo.com).

K. Hussain is with the Mechanical Engineering Department of Bradford University, UK, BD7 1DP (e-mail: K.Hussain1@bradford.ac.uk).

M. Layeghi is with the Dept. of wood & Paper Science & Technology, University of Tehran, Karaj, Tehran (email: mlayeghi@ut.ac.ir).

S. Sadeghi is with the Niroo research Institute, Tehran, Iran (email: Saeed@me.iut.ac.ir).

In order to maintain this cycle, a liquid must be returned back to its original location. This can be easily achieved by utilization the wick material. The liquid droplets are absorbed by the wick and due to the capillary force provided by the porous media the fluid is returned back to the evaporator section [2].

One of the limitations of heat pipes performance which does not cause a failure but bounds the heat transfer rate, is the limitation owing to transport properties of the working fluid such as its thermal conductivity. One of the most advanced methods to improve the thermal conductivity of heat pipes working fluid is the dispersion of Nano scale solid particles into plane fluid (hence the name "Nano-fluids"). Since the thermal conductivity of solid materials is higher than fluids, therefore the mixture will have a higher overall thermal conductivity.

Xuan and Li [3] classify the possible reasons of thermal conductivity improvement of nanofluids as follows:

(1) Increase in effective surface area of heat flux absorbent.

(2) Increase in effective thermal conductivity of the fluid.

(3) Particles random interaction and collision.

(4) Unstructured flow geometry due to higher turbulence possibility in presence of nanoparticles.

Numerous experimental and analytical investigations on Nano-fluid have been reported in the literature. Kang et al., [4] investigated the effect of silver Nano fluid with a concentration of 1 mg/litre to 100 mg/litre and 35 nm particle size in diameter, on the performance of a circular grooved-heat pipe. Temperature distribution on evaporator and condenser section and subsequently the thermal resistance of the heat pipe using Nano-fluid and DI-water as working fluid was compared. Their results show that for the input power range of 30 to 60 watt the thermal resistance decreased by 10-80%. They have also declared that there is a negative correlation between thermal resistance and Nano particles size.

Kang et al., [5] employed the same experimental test that they did in 2006 to investigate the effect of silver nanofluid with the same particle concentration and dimension on a sintered heat pipe. Their results indicate that the temperature difference in evaporator and condenser sections drops to 0.56-0.65 C°. Furthermore, the pipe filled with silver Nano fluids has the ability to transfer heat up to 70 watt while its counterpart with DI-water as working fluid is limited to 20 watt. Wang et al., [6] studied the CuO Nano fluid working fluid effect both in steady operation process and start up conditions. According to their achievement, in the start-up conditions nanofluid implementation drastically reduces the response time of the heat pipe.

Nomenclature

A	Surface area $[m^2]$
C_p	Specific heat $[J/(Kg.K)]$
h_{fg}	Latent heat of vaporisation $[J/Kg]$
K	Wick permeability $[m^2]$
k	Thermal conductivity $[W/(m.K)]$
k_{eff}	Saturated Wick Thermal Conductivity $[W/(m.K)]$
k_{layer}	Nanolayer thermal conductivity $[W/(m.K)]$
L	Length $[m]$
P	Pressure $[Pa]$
q	Input heat rate $[W]$
$q^{"}$	Heat flux $[w/m\text{^}2]$
R	Heat pipe thermal resistance, Gas constant $[K/W], [J/(mol.K)]$
R_{out}	Heat pipe outer radius $[m]$
r	Cylindrical coordinates $[m]$
r_p	Nanoparticle radius $[nm]$
S	Source term $[W/m\text{^}3]$
T	Temperature $[K]$
t	Pipe thickness $[mm]$
u	Horizontal velocity component $[m/s]$
v	Vertical velocity component $[m/s]$
w	Nanolayer Thickness $[nm]$
x	Cylindrical coordinates $[m]$

Greeks

φ	Nanoparticle concentration
ε	Wick porosity
μ	Dynamic viscosity $[(N.s)/m\text{^}2]$
ρ	Density $[Kg/m\text{^}3]$

Subscript

a	adiabatic
bf	Base fluid
c	condenser
e	evaporator
eff	effective
Int	interface
l	liquid
max	maximum
min	minimum
nf	nanofluid
P	particle
s	solid
sat	saturation
v	vapour

Superscript

$-$	Average quantity

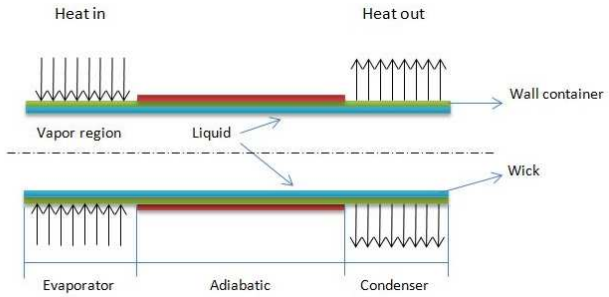

Fig. 1 Cylindrical heat pipe schematic

Besides the heat transfer capacity increases by 40% as well as a significant reduction in thermal resistance of the heat pipe by approximately 50%. A mathematical model of a cylindrical heat pipe using Al2O3, CuO and TiO2 nanofluids was solved analytically by Shafahi et al., [7]. The effect of nano fluid in their analytical study applied by using the mathematical model of effective heat conductivity; introduced by Yu and Choi [8,9]. Numerous interesting points were dazzling in the analysis outcomes such as the smaller particle size, the more pronounced effect on the evaporator/condenser temperature difference. Also they have proven that there is an optimum mass concentration which restricts the amount of removed heat load. Lastly the heat pipe thermal resistance falls as the mentioned nanofluids are utilized as heat pipe working fluid comparing to water which agrees with previous experimental works.

Liu [10] used nanofluid which was a mixture of CuO with DI-water with average diameter of 50 nm. A horizontal mesh wick of a cylindrical heat pipe was used. According to the outcome of the study, once the heat pipe reached to the steady state condition, it was observed that the heat transfer coefficient both in evaporator and condenser improved, as well as the total transferred heat flux. Another important varied factor by the heat transfer coefficient increase is the decrease of the pressure under sub-atmospheric operating condition of the pipe.

In this study the effect of nanofluids controllable factors (e.g. particle concentration level, size and material) on the thermal performance of a heat pipe was investigated using ANSYS-FLUENT commercial CFD package. The effect of nanoparticles on a circular heat pipe working fluid was investigated using the nanofluids thermal conductivity mathematical model proposed by Yu and Choi [8, 9]. To do so, it was assumed that the nanoparticles and the base fluid are in thermal equilibrium and the relative velocity of suspended particles and the bulk fluid is zero. The temperature distribution along the heat pipe wall and the system thermal resistance was assessed.

II. Mathematical Model and Governing Equations

For a heat pipe simulation the continuity, momentum, and energy equations are solved in cylindrical coordinates. The three-dimensional model can be reduced to two-dimensional due to no changes of flow characteristics in θ direction. The steady conditions will be the state of interest for the heat transfer and flow. Since it is assumed that each phase is fully saturated; continuity, momentum, and energy equations are solved for vapour and liquid regions separately using ANSYS-FLUENT software. The Darcy's law was used to govern the momentum equations for the fluid flow in porous media. Subsequently in order to apply the effect of latent heat of vaporization, numerical effect of a heat source term added to evaporator and condenser sections. Both phases of the fluid are assumed to be incompressible along with constant properties as well as laminar motion [11].

The method of solution for complex geometry involves discretization of the continuous domain into numerous elements and a solution of the flow/heat characteristics was found for each element of the domain using SIMPLE algorithm.

For the vapour region, the continuity, momentum and energy equation can be written as follows:

$$\frac{\partial u_v}{\partial x}+\frac{\partial v_v}{\partial r}+\frac{v_v}{r}=0 \tag{1}$$

$$\rho_v\left(u_v\frac{\partial u_v}{\partial x}+v_v\frac{\partial u_v}{\partial r}\right)= -\frac{\partial P_v}{\partial x}+\mu_v\left(\frac{4}{3}\frac{\partial^2 u_v}{\partial x^2}+\frac{1}{r}\frac{\partial}{\partial r}\left(r\frac{\partial u_v}{\partial r}\right)+\frac{1}{r}\frac{\partial}{\partial r}\left(r\frac{\partial v_v}{\partial r}\right)-\frac{2}{3}\frac{\partial}{\partial x}\left(\frac{1}{r}\frac{\partial}{\partial r}(rv_v)\right)\right) \tag{2}$$

$$\rho_v\left(u_v\frac{\partial v_v}{\partial x}+v_v\frac{\partial v_v}{\partial r}\right)= -\frac{\partial P_v}{\partial r}+\mu_v\left(\frac{\partial^2 u_v}{\partial x^2}+\frac{4}{3r}\frac{\partial}{\partial r}\left(r\frac{\partial v_v}{\partial r}\right)-\frac{4}{3}\frac{v_v}{r^2}\left(r\frac{\partial v_v}{\partial r}\right)+\frac{1}{3}\frac{\partial^2 u_v}{\partial x\partial r}\right) \tag{3}$$

$$\rho_v C_{p,v}\left(u_v\frac{\partial T_v}{\partial x}+v_v\frac{\partial T_v}{\partial r}\right)=\frac{k_v}{r}\left[\frac{\partial}{\partial r}\left(r\frac{\partial T_v}{\partial r}\right)+r\frac{\partial^2 T_v}{\partial x^2}\right]+v_v\frac{\partial P_v}{\partial r}+u_v\frac{\partial P_v}{\partial x} \tag{4}$$

The radial vapour and suction velocities boundary condition in all three sections of heat pipe at the vapour-liquid interface is given by [12]:

$$v_e=+\frac{q}{2\pi R_{Int}L_e\rho_v h_{fg}}$$
$$v_a=0 \tag{5}$$
$$v_c=-\frac{q}{2\pi R_{Int}L_c\rho_v h_{fg}}$$

The vapour-liquid interface temperature for all sections is calculated using Clausius-Clapeyron formula [13]:

$$T_{Int}=\frac{1}{\frac{1}{T_{v,sat}}-\frac{R}{h_{fg}}\ln\frac{P_v}{P_{v,sat}}} \tag{6}$$

For the wicking material the Darcy's law for fluid mass transport in porous media has been utilized to derive the momentum equations:

$$\rho_l\left(u_l\frac{\partial u_l}{\partial x}+v_l\frac{\partial u_l}{\partial r}\right)=-\frac{\partial P_l}{\partial x}+\mu_l\left(\frac{\partial^2 u_l}{\partial x^2}+\frac{1}{r}\frac{\partial}{\partial r}\left(r\frac{\partial u_l}{\partial r}\right)\right)-\frac{\mu\varepsilon_x u_l}{K_x} \tag{7}$$

$$\rho_l\left(u_l\frac{\partial v_l}{\partial x}+v_l\frac{\partial v_l}{\partial r}\right)=-\frac{\partial P_l}{\partial r}+\mu_l\left(\frac{\partial^2 v_l}{\partial x^2}+\frac{1}{r}\frac{\partial}{\partial r}\left(r\frac{\partial v_l}{\partial r}\right)\right)-\frac{\mu\varepsilon_r u_l}{K_r} \tag{8}$$

The energy equation in porous media may be defined as:

$$\rho_v C_{p,l}\left(u_l\frac{\partial T_l}{\partial x}+v_l\frac{\partial T_l}{\partial r}\right)=\frac{k_{eff}}{\varepsilon}\left[\frac{1}{r}\frac{\partial}{\partial r}\left(r\frac{\partial T_l}{\partial r}\right)+\frac{\partial^2 T_l}{\partial x^2}\right]+S \tag{9}$$

The values of the source terms which are applied to evaporator and condenser sections in order to include the phase change phenomenon are [11]:

$$S_e=-\frac{q}{\pi((R_{Int}+t)^2-R_{Int}{}^2)L_e}$$
$$S_c=+\frac{q}{\pi((R_{Int}+t)^2-R_{Int}{}^2)L_c} \tag{10}$$

And k_{eff} is the effective thermal conductivity of the saturated wick [1].

$$k_{eff}=\frac{k_{nf}\left[\left(k_{nf}+k_s\right)-(1-\varepsilon)\left(k_{nf}-k_s\right)\right]}{\left[\left(k_{nf}+k_s\right)+(1-\varepsilon)\left(k_{nf}-k_s\right)\right]} \tag{11}$$

Where k_{nf} may be presented by the mathematical model of the nanofluids effective thermal conductivity suggested by [8, 9] and adopted in this study:

$$k_{nf}=\frac{k_{Pe}+2k_l+2(k_{Pe}-k_l)(1-\beta)^3\varphi}{k_{Pe}+2k_l-2(k_{Pe}-k_l)(1+\beta)^3\varphi}k_b \tag{12}$$

Where k_{Pe} may be calculated from:

$$k_{Pe}=\frac{[2(1-\alpha)+(1+\beta)^3(1+2\alpha)\alpha]}{-(1-\alpha)+(1+\beta)^3(1+2\alpha)}K_l \tag{12a}$$

And

$$\alpha=\frac{k_{layer}}{k_p}\quad\&\quad\beta=\frac{w}{r_P} \tag{12b}$$

Where α is the ratio of nanolayer and the solid particles thermal conductivity, and β is the ratio of the thickness of nanolayer and the radius of the particle itself. The main advantage of this model is its ability to link the nanofluid thermal conductivity to particle size.

Moreover Brinkman [14] classical model is used to predict the density and viscosity of Nano fluids:

$$\rho_{nf} = \rho_P \varphi + (1-\varphi)\rho_{bf} \tag{13}$$

$$\mu_{nf} = \frac{\mu_{bf}}{(1-\varphi)^{2.5}} \tag{14}$$

Eventually the value of the heat flux over each section of the pipe may be calculated using the following:

$$\begin{aligned} q''_e &= + \frac{q}{2\pi R_{out} L_e} \\ q''_a &= 0 \\ q''_c &= - \frac{q}{2\pi R_{out} L_c} \end{aligned} \tag{15}$$

III. Model Dimension & Mesh Properties

A two dimensional axisymmetric model for the heat pipe was constructed in GAMBIT pre-processor software. The length of the modelled heat pipe is 1000 mm while its outer diameter is 33.5 mm. The evaporator and condenser sections have a length of 200 and 250 mm. The pipe container wall and wick thickness are 4.07 and 3.7 mm respectively (see Fig. 2.).

Once the geometry was constructed the mesh generation process was then carried by defining the grid points on each edge. Subsequently quadrilateral elements were created on the model-faces using the "Mapped Mesh" scheme. The total numbers of nodes created for the model were 43,611 nodes which were used to discretise the continuous domain.

Due to the presence of partial vacuum in the pipe, the temperature at which water starts to be vaporised is less than that at ambient pressure. It is assumed that the working temperature of heat pipe is 338 K. According to water vapour thermodynamic tables the working pressure at 338 K is 25030 Pascal. The thermo physical properties of the liquid in both phases were used for the ANSYSY-FLUENT software at this pressure. The simulation was exposed to 450 watt input heat load to evaporator and the heat pipe container and wick material was selected as copper.

IV. Result and Discussion

The dominant methodology which has been used to investigate the influence of nanofluids on a heat pipe performance is to compare the overall heat pipe thermal resistance using base/nanofluid as the working fluid. Heat pipe thermal resistance may be calculated from equation (16).

$$R = \frac{\overline{T_e} - \overline{T_c}}{q} \tag{16}$$

Where

$$\overline{T_e} = \frac{T_{e,max} + T_{e,min}}{2} \tag{17a}$$

$$\overline{T_c} = \frac{T_{c,max} + T_{c,min}}{2} \tag{17b}$$

The target of the study focuses on investigation of heat pipe thermal performance in presence of nanoparticles. In addition, the effect of changing nanofluid parameters (e.g. particle concentration, size and thermal conductivity) was directly examined on heat pipe wall temperature distribution, system thermal resistance as well as liquid velocity and pressure.

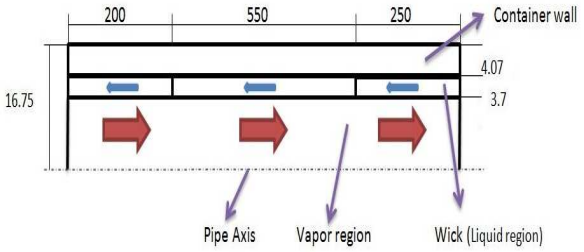

Fig. 2 Modeled heat pipe dimension (in mm)

A. Nanoparticle Concentration Level

To determine a comprehensive correlation for the thermal resistance of a heat pipe filled with Nano fluid with reference to the nanoparticle concentration, the effect of several concentration levels were investigated on the heat pipe wall temperature variation. The particles material selected was Alumina (Al_2O_3). Fig.3. shows the temperature changes with reference to different nanoparticle concentration. By increasing the nanoparticle accumulation, the temperature gradient in evaporator and condenser becomes less. This happens mainly due to the direct relation of particles concentration with the nanofluid thermal conductivity.

As the particle concentration raises (i.e. effective thermal conductivity of the working fluid increases) the temperature amplitude drops in the evaporator section. This happens owing to the higher heat flux passes through wick layer as the fluid thermal conductivity increases.

In this case because of the higher amount of transmitted heat flux along adiabatic and condenser sections the temperature on these segments increase by growing the particle concentration. Subsequently the descent pattern of thermal resistance as the concentration grows can be found in Fig.4. As far as the liquid pressure is concerned a nonlinear pattern in pressure gradient is noticeable. It can be observed from Fig.5 that by increasing the amount of particle concentration by 3% initially the pressure difference decreases. This behaviour reverses once the concentration level reaches to a specific value and beyond. The nonlinear trend of liquid pressure may be justified by the conflicting roles of density and viscosity growth while concentration

increases. Initially the raise in fluid density overcomes the viscosity effect and hence less pressure gradient occurs in liquid phase. However once the accumulation level passes the critical limit, the influence of viscosity outweighs the density increase and causes higher shear stress produced by the liquid in the porous region.

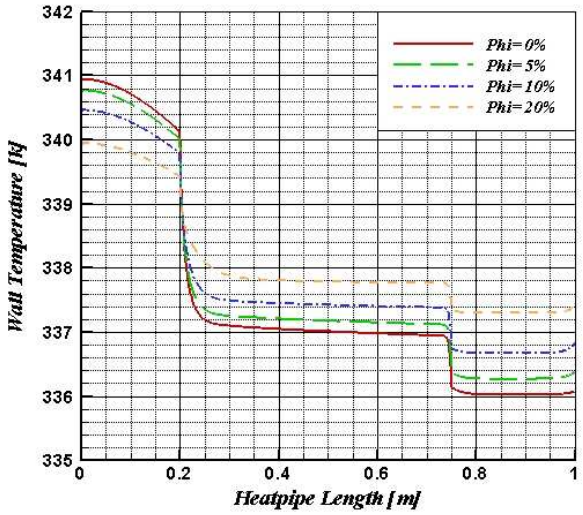

Fig. 3 Heat pipe wall temperature distribution with reference to various particle concentration levels

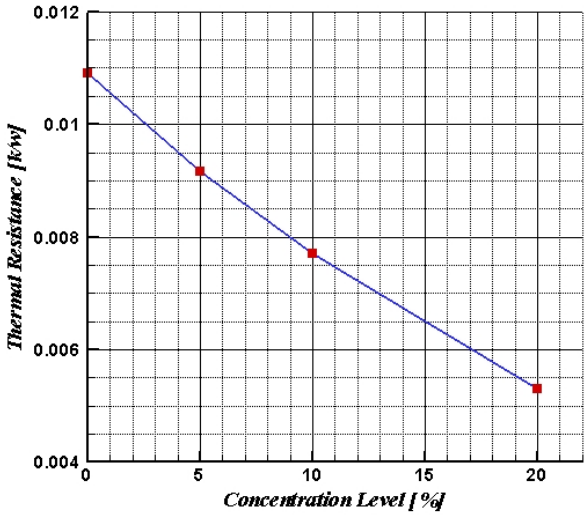

Fig. 4 Heat pipe Thermal resistance with reference to various particle concentration levels

The opposite effect of density and viscosity leads to appearance of the critical concentration.

Another effect of the particle concentration is on the liquid velocity. Because of the increase in fluid density by adding more nanoparticles, it is expected to see a slower liquid flow through the wick structure. The result of the liquid axial velocity changes for various concentration levels are illustrated in Fig.6.

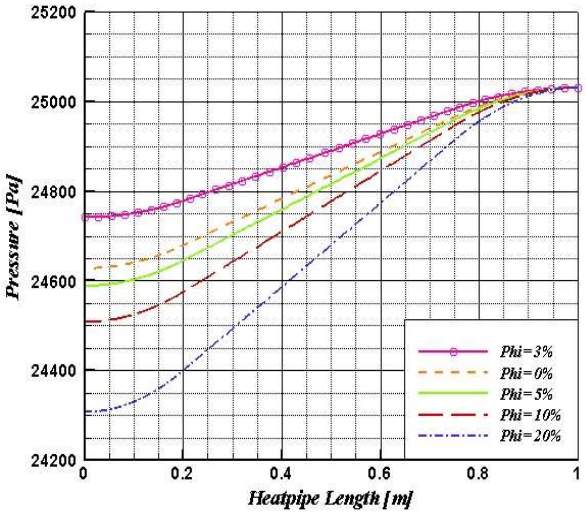

Fig. 5 Liquid pressure distribution in wick with reference to various particle concentration levels

B. Nanoparticle Size

Since the size of the nanoparticles can be treated as variable, the effect of this parameter on a heat pipe performance was also investigated. In order to apply the particle size modifications into the numerical model, the radius of spherical geometric Alumina particles is set to 10, 30, 50 and 100 Nano meters with a fixed particle concentration level at 10 %. The wall temperature variations with respect to different nanoparticle size are presented in Fig.7.

The Figure clearly highlights that by decreasing the particle size within the fluid, the heat pipe wall temperature distribution reduces. The reason for this reduction can be explained by the higher velocity of smaller particles which enhances the likelihood of fragments collision. The higher rate of impact among the particles causes a quasi-convection state to be formed between the bulk fluid molecules and nanoparticles and hence the overall thermal conductivity of the fluid was improved. Besides by shrinkage the particle size the overall effective liquid/solid phase interfacial area expands which assists the effective thermal conductivity to be enriched.

Once the effective thermal conductivity of the system is increased, the local temperature rise in evaporator section is reduced owing to the less heat flux accumulation on the wall.

Additionally the increase in adiabatic and condenser sections temperature with respect to the particle size reduction is due to the higher amount of heat which is transferred through these sections.

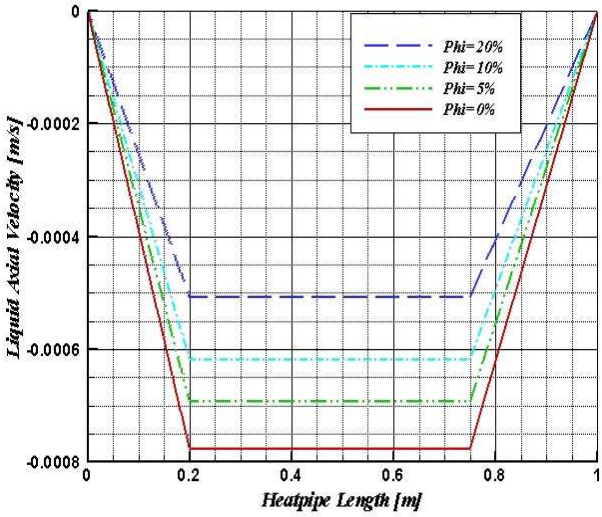

Fig. 6 Liquid axial velocity in wick with reference to various particle concentration levels

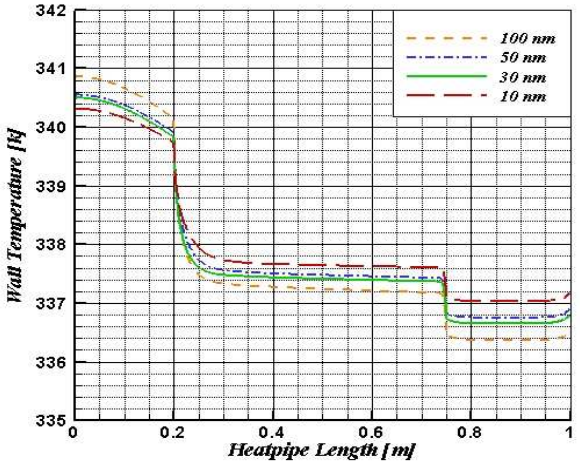

Fig. 7 Heat pipe wall temperature distribution with reference to various nanoparticle sizes

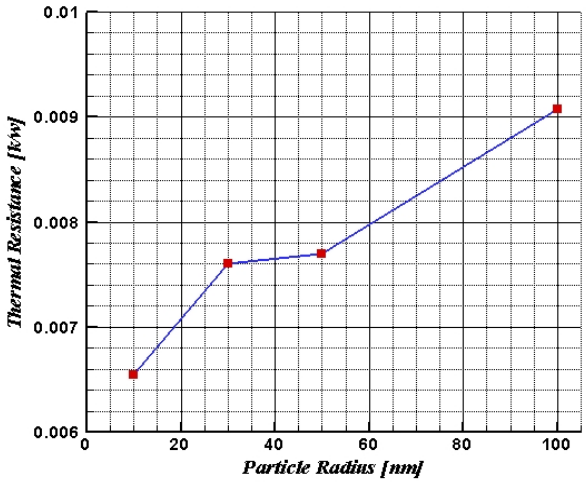

Fig. 8 Heat pipe Thermal resistance with reference to various particle sizes

C. Nanoparticle Substance

The effect of Nano particle material can be directly represented by the nanoparticle thermal conductivity. Since the thermal conductivity of nanofluids is a linear function of nanoparticle thermal conductivity (see equation 11), it is expected to observe different temperature distribution along the pipe while the nanoparticle substance varies. In this instance three different nanoparticles which are Titanium Dioxide (TiO_2), Alumina (Al_2O_3) and Copper (Cu) have been considered. The particle concentration level maintained at 10% and the particles radius was 50 nm.

Fig.9. represents the heat pipe outer wall temperature profile with reference to different nanoparticle materials. The results ascertain that the thermal conductivity of nanoparticle is directly correlated to the amount of temperature difference at both evaporator and condenser segments of the pipe. It can be noted that the least temperature difference along the pipe belongs to the Copper nanoparticle which has the highest thermal conductivity amongst the selected substances. In addition, the most temperature difference in presence of nanofluid is the result of using Titanium Dioxide as the suspended nanoparticles in the base fluid.

Fig.10. shows that the change of system thermal resistance by altering the particle material. With increasing the thermal conductivity of the nanoparticle the thermal resistance drops correspondingly. The peak of the graph is related to the thermal resistance of the system utilising base fluid and the lowest point is the result of using Copper-water Nano fluid as the heat pipe working fluid.

V. Conclusion

In this study the thermal performance of a cylindrical heat pipe was numerically simulated in presence of nanofluids using ANSYS-FLUENT commercial CFD package. The effects of Cu, TiO_2 and Al_2O_3 water based nanofluids on heat pipe wall temperature distribution, thermal resistance, liquid pressure and velocity with reference to various particle sizes and concentrations were explored.

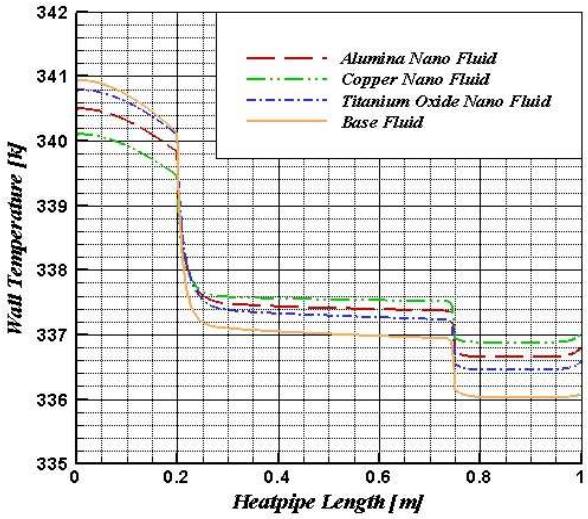

Fig. 9 Heat pipe wall temperature distribution with reference to different particle substances

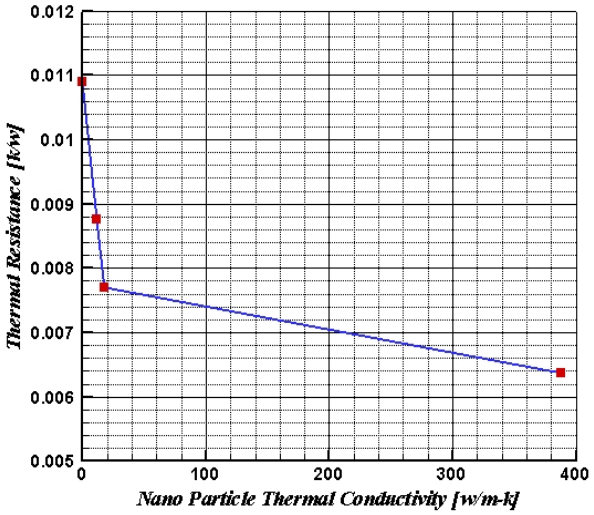

Fig. 10 Heat pipe Thermal resistance with reference to various particle substances

The results of the simulation showed the positive influence of nanofluid utilising as a heat pipe working fluid on the system thermal performance. It was found that by increasing the particle concentration level and particle thermal conductivity, the thermal resistance of the heat pipe reduces. Besides, the reduction in particle size leads to improve heat pipe thermal performance. As far as the liquid axial velocity (in wick structure) is concerned, a fall in velocity magnitude was observed as the particle concentration level increases. Lastly the effect of concentration on liquid pressure was studied. It was seen that the opposite role of nanofluid density and viscosity causes the presence of specific concentration level so called “critical concentration”.

REFERENCES

[1] Amir Faghri, Heat pipe science and technology, Taylor & Francis publishing, Oxon, 1995.
[2]] R. R. Williams. D. K. Harris, The heat transfer limit of step-graded metal felt heat pipe wicks. International Journal of Heat and mass transfer 48 (2005) 293-305.
[3] Y. Xuan, Q. Li, Heat transfer enhancement of nanofluids, Intenational Journal of Heat and Fluid Transfer 21 (2000) 58-64.
[4] S.-W. Kang, W.-C. Wei, S.-H. Tsai, S.-Y. Yang, Experimental Investigation of Silver nanofluid on Heat Pipe Thermal Performance, Applied Thermal Engineering 26 (2006) 2377-2382.
[5] S.-W. Kang, W.-C. Wei, S.-H. Tsai, S.-Y. Yang, Experimental Investigation of nanofluids on Sintered Heat Pipe Thermal Performance, Applied Thermal Engineering 29 (2009) 937-979.
[6] G.-S. Wang, B. Song, Z.-H. Liu, Operation Characteristics of Cylindrical Miniature Grooved heat Pipe Using Aqueous CuO nanofluids. Experimental Thermal and Fluid Science 34 (2010) 1415-1421.
[7] M. Shafahi, B. Vincenzo, K. Vafai, O. Manca, An Investigation of Thermal Performance of Cylindrical Heat Pipes Using nanofluids. International Journal of Heat and Mass transfer 53 (2010) 376-383.
[8] S.K. Das, S.U.S. Choi, W. Yu, T. Pradeep, Nanofluids science and Technology, John Wiley & Sons, Hoboken, 2008.
[9] W. Yu, S.U.S Choi, The role of interfacial layers in the enhanced thermal conductivity of nanofluids: a renovative Maxwell model, J, Nanoparticle Res. 5 (2003) 167-171.
[10] Z. Liu, Q. Zhu, Application of Aqueous Nano Fluids in a Horizontal Mesh Heat Pipe. Energy Conservasion and Management 52 (2011) 292-300.
[11] S. Mahjoub, A. Mahtabroshan, Numerical Simulation of A Conventional Heat Pipe. World Academy of Science, Engineering and Technology 39 (2008) 117-122.
[12] N. Zhu, K. Vafai, Analysis of cylindrical heat pipes incorporating the effects of liquid-vapor coupling and non-darcian transport- a closed form solution. In. J. of Heat and Mass Transfer 42 (1999) 3405-3418.
[13] A. Nouri-Boroujerdi, M. Layeghi, Numerical analysis of vapour flow in concenteric annular heat pipes. Transaction of ASME: Journal of Heat Transfer 162 (2004) 442-448.
[14] H.C. Brinkman, The viscosity of concentrated suspensions and solution, J. Chem. Phys. 20 (1952) 571-581.
[15] M. Keshavarz-Moraveji, M. Darabi, S. M. Haddad, R. Davarnejad, Modeling of Convection Heat transfer of a nanofluid in the Developing Region of tube flow with computational fluid dynamics. International Communications in Heat and Mass Transfer 42 (2011) 73-78.